JITTER PROBABILITY IN THE BREAKPOINTS OF DISCRETE SPARSE PIECEWISE-CONSTANT SIGNALS

Jorge Muñoz-Minjares, Jesús Cabal-Aragón, Yuriy S. Shmaliy

Department of Electronics Engineering, Universidad de Guanajuato
Ctra. Salamanca-Valle, 3.5+1.8km, Palo-Blanco, 36855, Salamanca, Mexico
phone: + 52 (464) 647-99-40, email: shmaliy@ugto.mx,
web: www.ingenierias.ugto.mx

ABSTRACT

It is shown that jitter is fundamentally inherent to the breakpoints of discrete sparse piecewise-constant signals measured in noise. No one estimator, even ideal, is able to provide the jitter-free breakpoints detection with unit probability. Even so, the jitter distribution in such signals was unknown so far. We have shown that for noise having white properties the jitter can be approximated with the discrete skew Laplace distribution irrespective of the segmental distributions. The theory was tested in Gaussian and heavy-tailed Cauchy noise environments and good correspondence was demonstrated.

1. INTRODUCTION

A great deal of applied problems meet a necessity of recovering different kinds of piecewise-constant signals from noisy measurements. Such a signal is sparse with a limited number of breakpoints between constant segmental levels. In applications, it occurs both intentionally, by modulation, and naturally, by undergoing processes. One classical example is the compound Poisson process [1] and another one is the Haar-based signal forming and representation. We find piecewise constant signals in digital message transmission, power line communications [2], genome copy number variations [3], and Markov chains. Images are also often composed of pieces having different colors with sharp edges.

To provide denoising while preserving edges in piecewise-smooth signals, several approaches have been developed during decades. A considerable interest has received nonlinear *wavelet*-based processing with thresholding [4–6] highly efficient in Gaussian noise. For heavy-tailed and Gaussian with outliers noise environments the *nonlinear smoothers* based on robust statistics were shown to have better performance [7–10]. Referring to the fact that time-variant linear structures are able to produce effects similar to the nonlinear ones, *adaptive* and *time-variant smoothers* were suggested and investigated in [11–14]. Also, the *forward-backward* (FB) filters and smoothers are used with this aim in engineering practice [15, 16].

Any estimate of a piecewise-constant (stepwise) signal measured in noise is accompanied with segmental errors and *jitter* in the breakpoints locations. Estimates of the constant segmental levels between the breakpoints are most accurately provided by averaging and well studied. However, jitter in the breakpoints still remains not well understood, although some investigations clearly demonstrate its existence [17]. Note that jitter in piecewise smooth signals has another nature than that in digital channels. Below we show that jitter
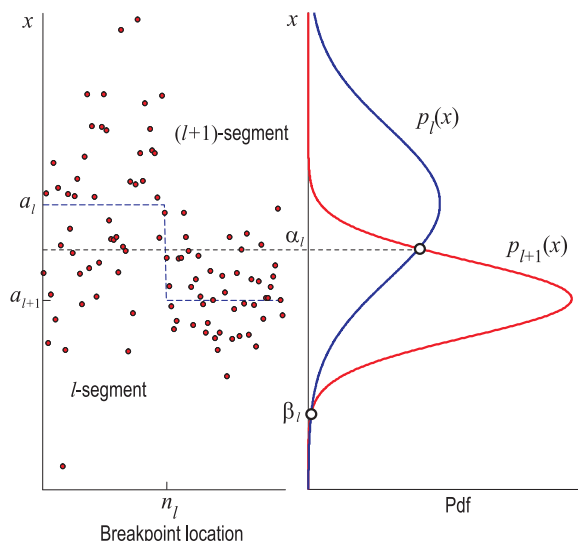
Figure 1: An example of a sparse (two-segment) discrete piecewise-constant signal measured in white Gaussian noise.

is fundamentally inherent to the breakpoints of piecewise-constant signals measured in white noise and that it can be represented approximately with the recently derived *discrete skew Laplace distribution* [18] irrespective of the segmental distributions.

2. JITTER PROBABILITY

A typical example of a sparse (two-segment) discrete piecewise-constant signal measured in white Gaussian noise is shown in Fig. 1. Here a constant signal changes from level a_l at point $n_l - 1$ to level a_{l+1} at point n_l that is called the *breakpoint*. Perturbed by noise, location of n_l is not clearly determined owing to commonly large segmental variances σ_l^2 and σ_{l+1}^2. As an example, the segmental noise probability density functions (pdfs) $p_l(x)$ and $p_{l+1}(x)$ are shown in Fig. 1 for $\sigma_l^2 > \sigma_{l+1}^2$. Let us add that $p_l(x)$ and $p_{l+1}(y)$ cross each other in two points, α_l and β_l, provided $\sigma_l^2 \neq \sigma_{l+1}^2$.

Now consider N points neighboring to n_l in each segment. We thus may assign an event $A_j \triangleq A_{lj}$ meaning that measurement at point $n_l - N \leqslant j < n_l$ belongs to the lth segment. Another event $B_j \triangleq B_{lj}$ means that measurement at $n_l \leqslant j < n_l + N - 1$ belongs to the $(l+1)$th segment. We think that a measured value belongs to one segment if the probability is larger than if it belongs to another segment. For example, any measurement point in the interval between

$\alpha \triangleq \alpha_l$ and $\beta \triangleq \beta_l$ (Fig. 1) is supposed to belong to the $(l+1)$th segment.

Following Fig. 1 and assuming different noise variances, the events A_{lj} and B_{lj} can be specified as follows:

$$\underset{n_l-N_l \leqslant j < n_l}{A_j} \text{ is } \begin{cases} (\alpha < x_j) \wedge (x_j < \beta), & \sigma_l^2 > \sigma_{l+1}^2, \\ x_j > \alpha, & \sigma_l^2 = \sigma_{l+1}^2, \\ \alpha < x_j < \beta, & \sigma_l^2 < \sigma_{l+1}^2, \end{cases} \quad (1)$$

$$\underset{n_l \leqslant j < n_l+N_l-1}{B_j} \text{ is } \begin{cases} \beta < x_j < \alpha, & \sigma_l^2 < \sigma_{l+1}^2, \\ x_j < \alpha, & \sigma_l^2 = \sigma_{l+1}^2, \\ (x_j < \alpha) \wedge (x_j > \beta), & \sigma_l^2 > \sigma_{l+1}^2. \end{cases} \quad (2)$$

The inverse events are $\bar{A}_j = 1 - A_j$ and $\bar{B}_j = 1 - B_j$.

Events A_j and B_j can be united into two product blocks

$$\mathbf{A} = \{A_{n_l-N} A_{n_l-N+1} \dots A_{n_l-1}\}, \quad (3)$$
$$\mathbf{B} = \{B_{n_l} B_{n_l+1} \dots B_{n_l+N-1}\}. \quad (4)$$

If $\mathbf{A}$ and $\mathbf{B}$ occur simultaneously, then jitter at n_l will never occur. However, there may be found some other events which do not obligatorily lead to jitter. We ignore such events and define approximately the probability $P(\mathbf{AB})$ of the jitter-free breakpoint as

$$P(\mathbf{AB}) = P(A_{n_l-N} \dots A_{n_l-1} B_{n_l} \dots B_{n_l+N-1}). \quad (5)$$

The inverse event $\bar{P}(\mathbf{AB}) = 1 - P(\mathbf{AB})$ can thus be called the *jitter probability*.

In white Gaussian noise, all the events are independent and (5) can be rewritten as

$$P(\mathbf{AB}) = P^N(A)P^N(B), \quad (6)$$

where, following (3) and (4), the probabilities $P(A)$ and $P(B)$ can be specified as, respectively,

$$P(A) = \begin{cases} 1 - \int\limits_{\beta_l}^{\alpha_l} p_l(x)dx, & \sigma_l^2 > \sigma_{l+1}^2, \\ \int\limits_{\alpha_l}^{\infty} p_l(x)dx, & \sigma_l^2 = \sigma_{l+1}^2, \\ \int\limits_{\alpha_l}^{\beta_l} p_l(x)dx, & \sigma_l^2 < \sigma_{l+1}^2, \end{cases} \quad (7)$$

$$P(B) = \begin{cases} \int\limits_{\beta_l}^{\alpha_l} p_{l+1}(x)dx, & \sigma_l^2 > \sigma_{l+1}^2, \\ \int\limits_{-\infty}^{\alpha_l} p_{l+1}(x)dx, & \sigma_l^2 = \sigma_{l+1}^2, \\ 1 - \int\limits_{\alpha_l}^{\beta_l} p_{l+1}(x)dx, & \sigma_l^2 < \sigma_{l+1}^2, \end{cases} \quad (8)$$

where $p_l(x)$ is any probability density function (pdf) descending monotonously to the left and to the right from the peak-value.

Let us now think that jitter occurs at a point $n_l \pm k$, $0 \leqslant k \leqslant N$, and assign two additional blocks of events $\mathbf{A}_k = \{A_{n_l-N} \dots A_{n_l-1-k}\}$ and $\mathbf{B}_k = \{B_{n_l+k} \dots B_{n_l+N-1}\}$. The probability $P_k^- \triangleq P(\mathbf{A}_k \bar{A}_{n_l-k} \dots \bar{A}_{n_l-1} \mathbf{B})$ that jitter occurs at the kth point to the left from n_l (left jitter) and the probability $P_k^+ \triangleq P(\mathbf{A} \bar{B}_{n_l+1} \dots \bar{B}_{n_l+k-1} \mathbf{B}_k)$ that jitter occurs at the kth

point to the right from n_l (right jitter) can thus be written as, respectively,

$$P_k^- = P^{N-k}(A)[1 - P(A)]^k P^N(B), \quad (9)$$
$$P_k^+ = P^N(A)[1 - P(B)]^k P^{N-k}(B). \quad (10)$$

By normalizing (9) and (10) with (6), we arrive at a function that turns out to be independent on N:

$$f(k) = \begin{cases} [P^{-1}(A) - 1]^k & , \quad k > 0, \quad \text{(left)} \\ 1 & , \quad k = 0, \\ [P^{-1}(B) - 1]^k & , \quad k > 0. \quad \text{(right)} \end{cases} \quad (11)$$

Further normalization of $f(k)$ to have a unit area leads to the pdf $p(k) = \frac{1}{\phi} f(k)$, where ϕ is the sum of the values of $f(k)$ for all k,

$$\phi = 1 + \sum_{k=1}^{N \to \infty} [\varphi^A(k) + \varphi^B(k)], \quad (12)$$

where $\varphi^A(k) = [P^{-1}(A) - 1]^k$ and $\varphi^B(k) = [P^{-1}(B) - 1]^k$.

Now observe that, in our approximation neglecting some undefined probabilities, function $f(k)$ converges with k only if $0.5 < \tilde{P} = \{P(A), P(B)\} < 1$. Otherwise, if $\tilde{P} < 0.5$, the sum ϕ is infinite, $f(k)$ cannot be transformed to $p(k)$, and the breakpoint cannot be detected. Considering the case of $0.5 < \tilde{P} = \{P(A), P(B)\} < 1$, we conclude that $\ln \tilde{P} < 0$, $\ln(1 - \tilde{P}) < 0$, and $\ln(1 - \tilde{P}) < \ln \tilde{P}$. Next, using a standard relation $\sum_{k=1}^{\infty} x^k = \frac{1}{x^{-1}-1}$, where $x < 1$, and after little transformations we bring (12) to

$$\phi = \frac{P(A) + P(B) - 1}{[1 - 2P(A)][1 - 2P(B)]}. \quad (13)$$

The approximate *jitter pdf* $p(k)$ can finally be found to be

$$p(k) = \frac{1}{\phi} \begin{cases} [P^{-1}(A) - 1]^{|k|} & , \quad k < 0, \\ 1 & , \quad k = 0, \\ [P^{-1}(B) - 1]^k & , \quad k > 0, \end{cases} \quad (14)$$

where ϕ is specified by (13) and $0.5 < P(A), P(B) < 1$. Accordingly, (14) can be used to find the *jitter probability*.

If we now substitute $q = P^{-1}(A) - 1$ and $d = P^{-1}(B) - 1$, find $P(A) = 1/(1+q)$ and $P(B) = 1/(1+d)$, and provide the transformations, we arrive at a conclusion that (14) is the *discrete skew Laplace pdf* recently derived in [18]:

$$p(k|d,q) = \frac{(1-d)(1-q)}{1-dq} \begin{cases} d^k, & k \geqslant 0, \\ q^{|k|}, & k \leqslant 0, \end{cases} \quad (15)$$

where $d = e^{-\frac{\kappa}{v}} \in (0,1)$ and $q = e^{-\frac{1}{\kappa v}} \in (0,1)$ and in which κ and $v > 0$ still need to be connected to (14).

Note that both (14) and (15) have peak-values at zero, $k = 0$. To move these distribution to the breakpoint n_l, just substitute k with $k - n_l$ and change k around n_l.

Now, in order to find the variables κ and v used in (15) in terms of (14), we consider (14) and (15) at $k = -1$, $k = 0$, and $k = 1$. By equating (14) and (15), we first obtain $\frac{(1-d)(1-q)d}{1-dq} = \frac{1}{\phi} \frac{1-P(B)}{P(B)}$ for $k = 1$ and $\frac{(1-d)(1-q)q}{1-dq} = \frac{1}{\phi} \frac{1-P(A)}{P(A)}$ for $k = -1$ that gives us

$$v = \frac{1 - \kappa^2}{\kappa \ln \mu}, \quad (16)$$

where

$$\mu = \frac{P(A)[1-P(B)]}{P(B)[1-P(A)]}.$$

For $k = 0$, we have $\frac{(1-d)(1-)}{1-dq} = \frac{1}{\phi}$ and transform it to the equation

$$x^2 - \frac{\phi(1+\mu)}{1+\phi}x - \frac{1-\phi}{1+\phi}\mu = 0,$$

which proper solution is

$$x = \frac{\phi(1+\mu)}{2(1+\phi)}\left(1 - \sqrt{1 + \frac{4\mu(1-\phi^2)}{\phi^2(1+\mu)^2}}\right) \qquad (17)$$

and which $x = \mu^{-\frac{\kappa^2}{1-\kappa^2}}$ gives us

$$\kappa = \sqrt{\frac{\ln x}{\ln(x/\mu)}}. \qquad (18)$$

By combining (16) with (18), we also get a simpler form for ν, namely $\nu = -\frac{\kappa}{\ln x}$.

Note that so far we made no assumptions about the distribution of the segmental white noise. That means that the discrete skew Laplace distribution (15) approximately characterizes jitter in the breakpoints of piecewise-constant signals measured in white noise having any distribution.

2.1 White Gaussian Noise

Let us now suppose that the segmental noise is white Gaussian. We thus introduce the segmental signal-to-noise ratios (SNRs) [19]

$$\gamma^- = \frac{\Delta^2}{\sigma_l^2}, \quad \gamma^+ = \frac{\Delta^2}{\sigma_{l+1}^2},$$

where $\Delta \triangleq \Delta_l = a_{l+1} - a_l$, substitute the Gaussian pdf $p_l(x) = \frac{1}{\sqrt{2\pi\sigma_l^2}}\exp\left\{-\frac{(x-a_l)^2}{2\sigma_l^2}\right\}$ to (7) and (8), provide the transformations, and rewrite (7) and (8) as

$$P(A) = \begin{cases} 1 + \frac{1}{2}[\operatorname{erf}(g^\beta) - \operatorname{erf}(g^\alpha)] & , \quad \gamma^- < \gamma^+, \\ \frac{1}{2}\operatorname{erfc}(g^\alpha) & , \quad \gamma^- = \gamma^+, \\ \frac{1}{2}[\operatorname{erf}(g^\beta) - \operatorname{erf}(g^\alpha)] & , \quad \gamma^- > \gamma^+, \end{cases} \qquad (19)$$

$$P(B) = \begin{cases} \frac{1}{2}[\operatorname{erf}(h^\alpha) - \operatorname{erf}(h^\beta)] & , \quad \gamma^- < \gamma^+, \\ 1 - \frac{1}{2}\operatorname{erfc}(h^\alpha) & , \quad \gamma^- = \gamma^+, \\ 1 + \frac{1}{2}[\operatorname{erf}(h^\alpha) - \operatorname{erf}(h^\beta)] & , \quad \gamma^- > \gamma^+, \end{cases} \qquad (20)$$

where $g^\beta = \frac{\beta-\Delta}{|\Delta|}\sqrt{\frac{\gamma^-}{2}}$, $g^\alpha = \frac{\alpha-\Delta}{|\Delta|}\sqrt{\frac{\gamma^-}{2}}$, $h^\beta = \frac{\beta}{|\Delta|}\sqrt{\frac{\gamma^+}{2}}$, $h^\alpha = \frac{\alpha}{|\Delta|}\sqrt{\frac{\gamma^+}{2}}$, $\operatorname{erf}(x)$ is the error function, $\operatorname{erfc}(x)$ is the complementary error function, and

$$\begin{aligned} \alpha, \beta &= \frac{a_l\gamma^- - a_{l+1}\gamma^+}{\gamma^- - \gamma^+} \mp \frac{1}{\gamma^- - \gamma^+} \\ &\times \sqrt{(a_l - a_{l+1})\gamma^-\gamma^+ + 2\Delta^2(\gamma^- - \gamma^+)\ln\sqrt{\frac{\gamma^-}{\gamma^+}}} \end{aligned}$$
(21)
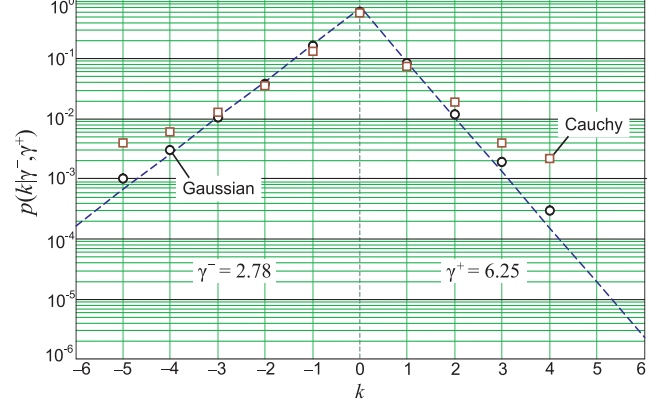
Figure 2: The jitter skew Laplace pdf (dashed) for different segmental SNRs; $k = 0$ corresponds to the actual breakpoint. Test measurements depicted with ○ and □ correspond to Gaussian and Cauchy noise environments, respectively. Discrepancies with large k are caused by the approximation.

if $\gamma^- \neq \gamma^+$. For $\gamma^- = \gamma^+$, set $\alpha = \Delta/2$ and $\beta = \pm\infty$.

The skew Laplace pdf (15) is shown in Fig. 2 for $\gamma^- = 2.78$ and $\gamma^+ = 6.25$. It predicts that jitter may occur at 5 points (three to the left and two to the right from $k = 0$) for the pdf level of 0.01. In order to verify (15) experimentally, we have simulated a piecewise-constant signal in white Gaussian noise with $\sigma_1 = 0.6$ and $\sigma_2 = 0.4$. To realize how (15) serves for non-Gaussian processes, we also simulated this signal in heavy-tailed Cauchy noise with the scale factors $s_1 = 0.2$ and $s_2 = 0.13$.

As can be seen, (15) serves well when noise is white Gaussian. In the Cauchy noise environment there is a good correspondence around $k = 0$. However, simulations reveal some tails beyond $k = 0$ that requires further investigations.

The jitter probability $P_k(\gamma^-, \gamma^+)$ can now be found utilizing (15). Because a step is unity in discrete k, the jitter probability $P_k(\gamma^-, \gamma^+)$ is given by

$$P_k(\gamma^-, \gamma_l^+) = p[k|d(\gamma_l^-, \gamma_l^+), q(\gamma_l^-, \gamma_l^+)]. \qquad (22)$$

Figure 3 sketches (22) for small and large equal SNRs $\gamma_1 = \gamma_2$. Here, we also show the probability of the jitter-free breakpoint detection (dashed) along with some preliminary simulations. As can be seen, (22) fits measurements and we may continue on with some analysis:

- When the SNRs are extremely small, the total jitter probability $P_J(\gamma^-, \gamma^+) = \bar{P}(\mathbf{AB})$ defined by (2) is almost unity. Herewith the probability of the jitter-free breakpoint detection (dashed) and the jitter probabilities at any other point naturally tend toward $\frac{1}{2N}$ (see that the relevant curves merge when γ^- and γ^+ tend toward zero).

- With an increase in the SNRs, the probability of the jitter-free breakpoint detection naturally becomes larger and finally reaches unity when $\gamma^- = \gamma^+ \to \infty$. On the other hand, the jitter probability at the kth point initially increases, then it reachs a maximum, and thereafter decreases to zero when $\gamma^- = \gamma^+ \to \infty$.

- It follows from Fig. 3 that the maximum jitter probability for $k = 1$ corresponds to about unit SNRs.

3
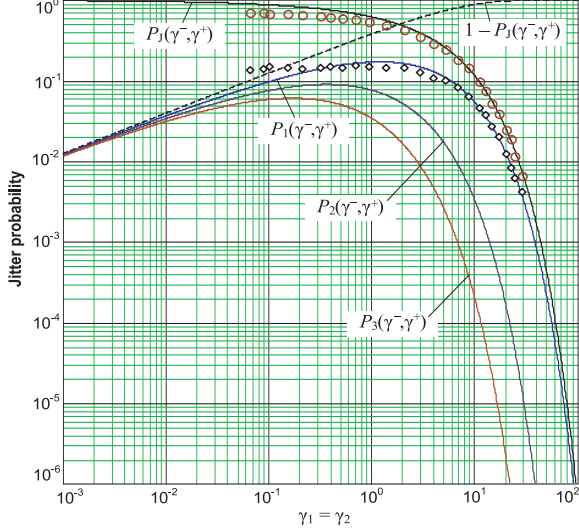
Figure 3: Total jitter probability $P_J(\gamma^-, \gamma^+)$ and probabilities $P_k(\gamma^-, \gamma^+)$ of the right jitter at $k = 1$, $k = 2$, and $k = 3$ for equal SNRs in the segments. The probability of the jitter-free breakpoint detection is dashed.

3. ESTIMATION OF BREAKPOINT LOCATION

The purpose of this section is to verify that jitter in the breakpoints exists fundamentally and depends strongly on the neighboring points as suggested by (14). Using (15), the jitter probability can be predicted for each k if the segmental variances σ_1^2 and σ_2^2 are known along with $\Delta = a_{l+1} - a_l$ (see Fig. 1). If to assume an ideal ML estimator, then the jitter probability (22) will characterize its output. Note that optimal and robust estimators do not add essential errors to the estimation of the breakpoint locations. Therefore, (12) may serve for real estimators in the lower bound sense. We have verified this statement at the early stage using the forward-backward smoother [16] and the averaging smoother [12].

3.1 Maximum Likelihood Estimation

To estimate the breakpoint locations shown in Fig. 2, Fig. 3, and below, the estimate $\hat{n}_l$ was found using the maximum likelihood (ML) estimator implying known segmental $a_l = 2$ and $a_{l+1} = 1$. We suppose that the measurement vector $\mathbf{y} \in \mathscr{R}^L$ is an additive sum of a signal vector $\mathbf{x}(n_l) \in \mathscr{R}^L$ and white noise vector $\mathbf{v} \in \mathscr{R}^L$. We then find $\hat{n}_l$ by minimizing the square $\mathscr{L}_2$-norm as

$$\hat{n}_l = \arg\min_{\hat{n}_l} \left(\frac{1}{2} \| \mathbf{y} - \mathbf{x}(\hat{n}_l) \|_2^2 \right), \qquad (23)$$

$$\text{Subject to } n_l - N < \hat{n}_l < n_l + N$$

where N is some reasonable number of points around n_l.

We now generate a piecewise-constant signal (Fig. 1) with $\sigma_1^2 = \sigma_2^2 = 0.25$ and $\Delta = 1$ that corresponds to $\gamma^- = \gamma^+ = 4$. Next, we change a location of the candidate breakpoint in the test signal with $N = 5$; that is, we handle the candidate breakpoint from $n = 46$ to $n = 56$. By using (23), we find $\hat{n}_l$ that is the ML estimate of the breakpoint location.

For the process simulated with $\gamma^- = \gamma^+ = 4$ the jitter probability $P_k = P_k(\gamma^-, \gamma^+)$ is predicted by (22) to be $P_0 = 68.3\%$, $P_1 = 12.9\%$, $P_2 = 2.4\%$, and $P_3 = 0.46\%$. Figure

4 sketches measurements and the estimates of the breakpoint location. It follows that an actual (jitter-free) breakpoint (Fig. 4a) is detected with $P_0 = 68.3\%$ and we notice that this probability is not large. We also give an example of a possible although quite rare ambiguity (Fig. 4b). In this case, the breakpoint is estimated to be located either at $k = -3$ with $P_{-3} = 0.46\%$ or at $k = 1$ with $P_1 = 12.9\%$.

Let us consider another example. Figure 5 gives several simulated examples of the genome copy number variations (CNVs) [20] with different realizations of the segmental white Gaussian noise. The case (a) is ideal to mean that with such locations of the measured points the estimate of the breakpoint i_l will always be *jitter-free*. If some points left-neighboring to i_l have happen to lie below the threshold (dashed), then the estimate will be found to the left of i_l; four points to the left in the case (b) represent the *left jitter*. If some right-neighboring points lie below the threshold, then the estimate will be found to the right of i_l; two points to the left in case (c) represent the *right jitter*. Also, there may be observed *ambiguities* as in case (d) when the estimator gives two or more possible locations of the same breakpoint. The latter case is akin to that shown in Fig. 4b. Practical applications of the jitter distribution derived are discussed in [21].

4. CONCLUSIONS

Jitter in the breakpoints is fundamentally inherent to sparse piecewise-constant signals measured in noise and is a strong limiter of accuracy with small segmental SNRs. In spite of this, the jitter distribution for such signals was unknown so far. We have derived and verified an approximate jitter distribution for signals measured in additive noise with white properties. We have also shown that this distribution is subject to the discrete skew Laplace law irrespective of the segmental distributions. An important applied significance of the jitter distribution derived resides in the fact that it allows forming the estimate upper and lower bounds. Such bounds are required in bioinformatics and other related fields implying measurements in large noise.

The jitter probability derived corresponds to the ideal ML estimator implying known segmental levels. It can also be used to characterize errors in real estimators in the lower bound sense. Simulations have confirmed the theory. The discrete Laplace distribution was shown to serve well around the breakpoints in white Gaussian noise environment, although some tails were revealed. We associate such tails with some unspecified and therefore neglected probabilities. Effect of the segmental noise distributions on the jitter probability and some critical applications are currently under investigation.

REFERENCES

[1] M. Unser and P. D. Tafti, "Stochastic models for sparse and piecewise-smooth signals," *IEEE Trans. Signal Process.*, vol. 59, pp. 989-1006, Mar. 2011.

[2] K. Dostert, *Power Line Communications*, Upper Saddle River, NJ: Prentice Hall, 2001.

[3] J. L. Semmlow, *Biosignals and medical image processing*, New York: CRC Press, 2009.

[4] D. L. Donoho, "De-noising by soft thresholding," *IEEE Trans. Inform. Theory*, vol. 41, pp. 613–627, Mar. 1995.
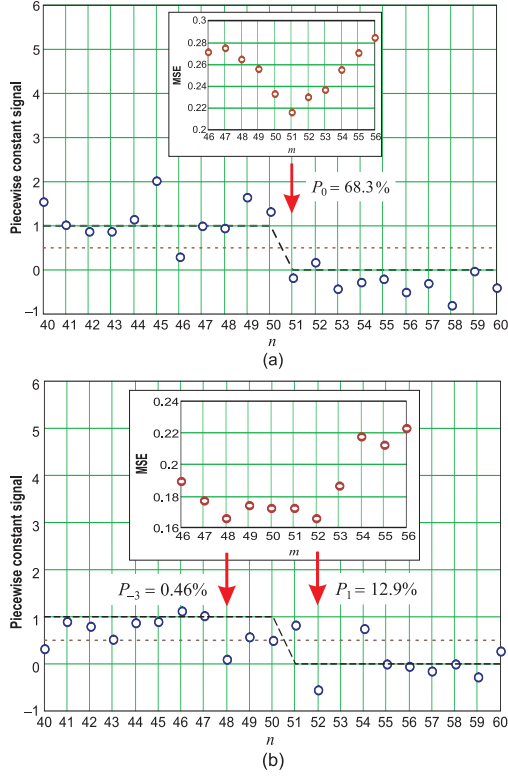
Figure 4: Measurements and ML estimates of the breakpoint location: (a) most probable jitter-free location with $P_0 = 68.3\%$ and (b) an ambiguity with $P_{-3} = 0.46\%$ and $P_1 = 12.9\%$.
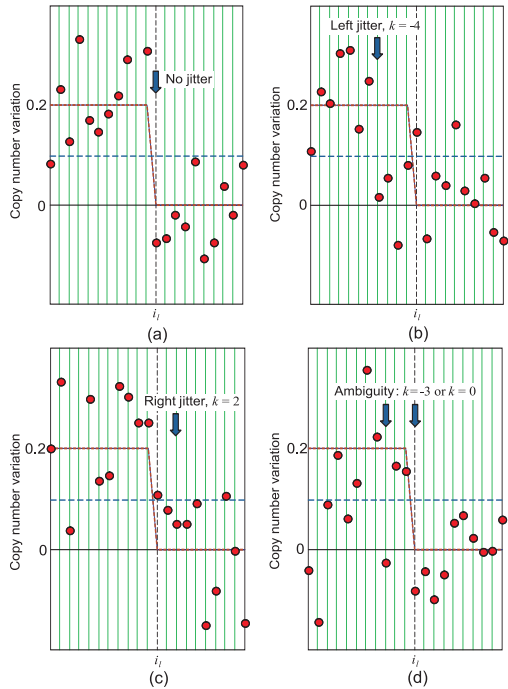
Figure 5: Effect of large noise on the CNVs measurements around the i_lth breakpoint: (a) ideal case – jitter-free, (b) left jitter at $k = -4$, (c) right jitter at $k = 2$, and (d) ambiguity at $k = -3$ or $k = 0$.

[5] X. P. Zhang and M. D. Desai, "Adaptive denoising based on SURE risk," *IEEE Signal Process. Let.*, vol. 5, pp. 265–267, Oct. 1998.

[6] S. G. Chang, B. Yu, and M. Vetterli, "Adaptive wavelet thresholding for image denoising and compression," *IEEE Trans. Image Process.*, vol. 9, pp. 1532–1546, Sep. 2000.

[7] J. W. Tukey, *Exploratory Data Analysis*, Menlo Park, CA: Addison-Wesley, 1971.

[8] D. R. K. Brownrigg, "The weighted median filter," *Commun. ACM*, vol. 27, pp. 807–818, Aug. 1984.

[9] S. Kalluri, G. R. Arce, "Adaptive weighted myriad filter algorithms for robust signal processing in α-stable environments," *IEEE Trans. Signal Process.*, vol. 46, pp. 322–334, Feb. 1998.

[10] G. R. Arce, *Nonlinear signal processing: a statistical approach*, New York: Willey 2005.

[11] O. V. Lepski, E. Mammen, V. G. Spokoiny, "Optimal spatial adaptation to inhomogenous smoothness: an approach based on kernel estimates with variable bandwidth selectors," *The Annals of Statistics*, vol. 25, pp. 929–947, Jun. 1997.

[12] J. Munoz-Minjares, O. Ibarra-Manzano, and Y. S. Shmaliy, "Maximum likelihood estimation of DNA copy number variations in HR-CGH arrays data," in *Proc. 12th WSEAS Int. Conf. on Signal Process., Comput. Geometry and Artif. Vision (ISCGAV'12), Proc. 12th WSEAS Int. Conf. on Systems Theory and Sc. Comput. (ISTASC'12)*, Istanbul, Turkey, 2012, pp. 45-50.

[13] A. Goldenshluger and A. Nemirovski, "Adaptive de-noising of signals satisfying differential inequalities," *IEEE Trans. Inf. Theory*, vol. 43, pp. 872–889, Mar. 1997.

[14] Y. S. Shmaliy and L. Morales-Mendoza, "FIR smoothing of discrete-time polynomial models in state space," *IEEE Trans. Signal Process.*, vol. 58, pp. 2544–2555, May 2010.

[15] B. D. Rao and K. V. S. Hari, "Effect of spatial smoothing on the performance of MUSIC and the minimum-norm method," *IEE Proc.*, vol. 137(F), no. 6, pp. 449–458, Dec. 1990.

[16] O. Vite-Chavez, R. Olivera-Reyna, O. Ibarra-Manzano, Y. S. Shmaliy, and L. Morales-Mendoza, "Time-variant forward-backward FIR denoising of piecewise-smooth signals," *Int. J. Electron. Commun. (AEU)*, vol. 67, pp. 406–413, May 2013.

[17] F. Picard, S. Robin, M. Lavielle, C. Vaisse, and J.-J. Daudin, "A statistical approach for array CGH data analysis", *BMC Bioinformatics*, vol. 6, pp. 1–14, Feb. 2005.

[18] T. J. Kozubowski and S. Inusah, "A skew Laplace distribution on integers", *Annals of the Inst. of Statist. Math.*, vol. 58, pp. 555-571, Sep. 2006.

[19] Y. S. Shmaliy, "On the multivariate conditional probability density of a signal perturbed by Gaussian noise", *IEEE Trans. on Inform. Theory*, vol. 53, pp. 4792-4797, Dec. 2007.

[20] P. Stankiewicz and J. R. Lupski, "Structural variation in the human genome and its role in disease," *Annual Review of Medicine*, vol. 61, pp. 437-455, Feb. 2010.

[21] J. Muñoz-Minjares, J. Cabal-Aragón, and Y. S. Shmaliy, "Probabilistic bounds for estimates of genome DNA copy number variations using HR-CGH microarray", in *Proc. 21st European Signal Process. Conf. (EUSIPCO-2013)*, Marrakech, Marocco, 2013.